Metabolic Engineering 48 (2018) 129–137

Contents lists available at ScienceDirect

Metabolic Engineering

journal homepage: www.elsevier.com/locate/meteng

Optimal bioprocess design through a gene regulatory network – Growth kinetic hybrid model: Towards replacing Monod kinetics

Argyro Tsipa[a], Michalis Koutinas[b], Chonlatep Usaku[a,c], Athanasios Mantalaris[a,*]

[a] Department of Chemical Engineering, South Kensington Campus, Imperial College London, London, United Kingdom
[b] Department of Environmental Science and Technology, Cyprus University of Technology, 30 Archbishop Kuprianou Str., Limassol, Cyprus
[c] Department of Biotechnology, Silpakorn University, Nakorn Pathom 73000, Thailand

ARTICLE INFO

Keywords:
P. putida
Bioprocess optimisation
Gene regulatory network
Mixed-substrate
Fed-batch
Monod Kinetics

ABSTRACT

Currently, design and optimisation of biotechnological bioprocesses is performed either through exhaustive experimentation and/or with the use of empirical, unstructured growth kinetics models. Whereas, elaborate systems biology approaches have been recently explored, mixed-substrate utilisation is predominantly ignored despite its significance in enhancing bioprocess performance. Herein, bioprocess optimisation for an industrially-relevant bioremediation process involving a mixture of highly toxic substrates, *m*-xylene and toluene, was achieved through application of a novel experimental-modelling gene regulatory network – growth kinetic (GRN-GK) hybrid framework. The GRN model described the TOL and *ortho*-cleavage pathways in *Pseudomonas putida* mt-2 and captured the transcriptional kinetics expression patterns of the promoters. The GRN model informed the formulation of the growth kinetics model replacing the empirical and unstructured Monod kinetics. The GRN-GK framework's predictive capability and potential as a systematic optimal bioprocess design tool, was demonstrated by effectively predicting bioprocess performance, which was in agreement with experimental values, when compared to four commonly used models that deviated significantly from the experimental values. Significantly, a fed-batch biodegradation process was designed and optimised through the model-based control of TOL *Pr* promoter expression resulting in 61% and 60% enhanced pollutant removal and biomass formation, respectively, compared to the batch process. This provides strong evidence of model-based bioprocess optimisation at the gene level, rendering the GRN-GK framework as a novel and applicable approach to optimal bioprocess design. Finally, model analysis using global sensitivity analysis (GSA) suggests an alternative, systematic approach for model-driven strain modification for synthetic biology and metabolic engineering applications.

1. Introduction

Until recently control of gene expression would be considered an ambitious yet futile endeavour. Nowadays the machinery of DNA, RNA and proteins are not only better understood, but also engineered to make useful products. The ever increasing importance of biotechnological applications and bioprocesses ranging from bioremediation to high-added value biologics production and cellular therapeutics biomanufacturing necessitates control and optimisation of the process of interest.

Pseudomonas putida is a metabolically versatile soil bacterium capable of thriving in diverse habitats that degrades a series of industrially significant pollutants (Timmis, 2002). The mt-2 strain encodes the TOL plasmid incorporating the molecular toolbox required for the degradation of aromatic compounds that belong to the toxic BTEX (benzene-toluene-ethylbenzene-xylene isomers) group of pollutants. Toluene and *m*-xylene are considered as the most common effectors of the TOL plasmid (pWW0) (Timmis, 2002), the degradation of which results in essential for biomass growth Krebs cycle intermediates. The TOL regulatory network of *P. putida* mt-2 has been previously described in detail (Ramos et al., 1997). In addition the TOL plasmid is considered a paradigm of global and targeted gene regulation due to the interplay between regulatory proteins, a group of sigma factors and DNA-bending proteins that control transcription from the system's catabolic operons constituting a complex regulatory gene network in its natural context (Aranda-Olmedo et al., 2005).

Bioprocess optimisation requires monitoring and prediction of bioperformance, use of mixed-substrates (Klecka and Maier, 1988; Lee and Huang, 2000), accounting for the dynamic nature of the biosystem, tailoring the feeding strategy of fed-batch/continuous processes, and scale-up through optimisation of bioreactor design. Traditionally, bioprocess optimisation is accomplished through laborious

* Correspondence to: Imperial College London, London SW7 2AZ, UK.
E-mail address: a.mantalaris@imperial.ac.uk (A. Mantalaris).

https://doi.org/10.1016/j.ymben.2018.04.023
Received 20 December 2017; Received in revised form 14 March 2018; Accepted 30 April 2018
Available online 02 May 2018

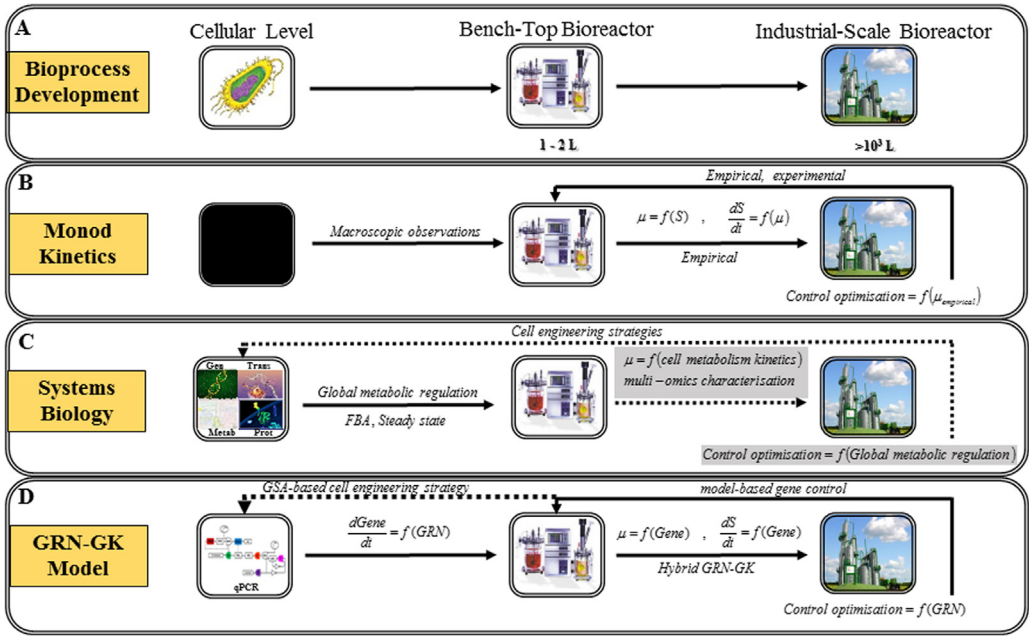

Fig. 1. (A) Bioprocess development from cellular to industrial-scale level driven by mathematical modelling employing: (B) Monod kinetics, (C) systems biology approaches, (D) the GRN-GK framework; : to be accomplished.

experimentation with the aid of mathematical expressions of microbial growth (Monod, 1949) which have been mainly developed for single substrate systems and employ unstructured Monod kinetics (Fig. 1). Monod-type models (Yano and Koga, 1969) are empirical and assume existence of a single metabolic reaction that follows Michaelis-Menten kinetics and which is responsible for substrate uptake. Models developed based on Monod expressions often lack fit and have narrow applicability, while ignoring transcriptional regulation (Kovarova-Kovara and Egli, 1998).

More recently systems biology approaches integrate "omics" methodologies and computational tools (Bartocci and Lió, 2016) to reconstruct genome-scale metabolic networks and attempt to predict growth kinetics (O'Brien et al., 2013), which in turn could potentially lead to system parts, control, optimisation and development of cell engineering and robustness strategies (Gerstl et al., 2016; Ranganathan et al., 2010). Genome-scale reconstruction is a time-consuming, experimentally-intensive, and mathematically challenging process that ultimately lacks predictability. Successful activation of metabolic networks relies on transcriptional regulation initiating the appropriate metabolic cascades. Significant progress on global gene regulatory network modelling has been achieved but these models are prohibitively complex, and reliable application of the approach remains an underdetermined computational problem (Banf and Rhee, 2017). Although genome-scale metabolic models may integrate transcriptomics data (Akesson et al., 2004), the data sets involved are insufficient and extracted using high-throughput technologies, such as microarrays and RNA-sequencing, which are often noisy, high dimensional and sparse, dramatically affecting quantitative analysis (Sławek and Arodz, 2013). Moreover, the typical steady-state assumption entailed ignores dynamic reality, often limiting the applicability of such models for optimal bioprocess design (Fig. 1). Whereas, recently the importance of kinetic genome-scale models has been recognised as a research toolkit in biosciences (Almquist et al., 2014; Chakrabarti et al., 2013; Jamshidi and Palsson, 2008), their applicability on scaling-up bioprocesses has not yet been rendered feasible.

Herein, we present the dynamic modelling of the GRN of the main metabolic pathway of *P. putida* mt-2 activated upon exposure to mixed-substrates. The GRN model utilised consistent, systematic time-series data of specific promoter(s) mRNA expression obtained through qPCR (Fig. 1). Subsequently, we efficiently connected the GRN model to growth kinetics (GK) resulting in prediction of mixed-substrates and growth patterns. The GRN-GK framework was utilised to predict optimal bioprocess design. It is versatile and can be rendered applicable to other host biological systems, including industrial microorganisms for which control and optimisation is essential to overcome various technological barriers encountered in full-scale applications. Finally, application of the framework on engineered GRNs may lead to predictable and robust bioprocess operation serving as an advanced synthetic biology tool with direct industrial applications in accelerating biomanufacturing and bioprocess scaling-up.

2. Materials and methods

2.1. Microbial cultures

Subcultures of *P. putida* mt-2 were pre-grown for 23 h at 30 °C in M9 minimal salts medium (Sambrook et al., 1989) supplemented with 10 mM of succinate. In each experiment, two independent cultures were prepared by diluting the overnight culture in minimal medium to an initial optical density of 0.1 (0.4 L working volume) measured at 600 nm (UV-2101PC, Shimadzu, UK) for every condition tested. The minimal medium was supplemented with toluene and *m*-xylene at the concentration level required in each experiment. Cultures were performed using conical Erlenmeyer flasks of 2.35 L total volume, which were continuously stirred at 1000 rpm via a Heidolph MR3001K (Heidolph, UK) magnetic stirrer. The flasks were filled with medium to one-sixth of their volume (0.4 L), to ensure that sufficient oxygen was available, and closed gas-tight with Teflon coated lids to avoid losses of the volatile organic compound. Temperature was maintained constant at 30 °C. All chemicals used were obtained from Sigma-Aldrich Company Ltd and were of ANALAR grade.

2.2. Substrate and biomass analyses

Gas Chromatograph (GC) analysis was employed for determination of *m*-xylene and toluene concentration in the gaseous and aqueous samples using an Agilent 6850 Series II Gas Chromatograph with a FID detector and a 'J&W Scientific' (Agilent Technologies UK Limited, UK) column with HP-1 stationary phase (30 m × 0.32 mm × 0.25 mm). Gaseous samples of 25 μL were injected into the GC and the temperature program run at 70 °C for 3 min and then increased to 80 °C at a rate of 5 °C min^{-1}. *m*-xylene and toluene concentration of the culture was

determined experimentally as previously described (Koutinas et al., 2010). Biomass concentration was determined by absorbance at 600 nm on a UV-1800 scanning spectrophotometer (Shimadzu, UK) interpolating from a previously established dry weight calibration curve. The coefficient of variation for 3 samples was 3.4% at a concentration level of 1233 $mg_{biomass}\ L^{-1}$.

2.3. Preparation and Isolation of Total RNA, cDNA Synthesis and qPCR

Culture samples of 3–4.5 ml (depending on cell density) were placed in cryogenic vials (Sigma-Aldrich Company Ltd, UK) and the cell pellet was harvested by centrifugation at 15000 rpm for 10 min at 4 °C. The supernatant was discarded and the vials were immersed in liquid nitrogen for 1 min and stored at − 80 °C until use. Real-Time Quantitative Polymerase Chain Reaction (qPCR) was performed to determine the expression of *xylR* (*Pr* promoter), *xylS* (*Ps* promoter), *xylU* (*Pu* promoter), *xylX* (*Pm* promoter), *benR* (*PbenR* promoter), *benA* (*PbenA* promoter) and *rpoN* (housekeeping) genes during the course of the experiments. The method for isolation of total RNA and cDNA synthesis has been previously described (Koutinas et al., 2010). The qPCR method as well as the calculation of relative mRNA expression based on threshold cycle values was conducted as previously (Koutinas et al., 2011, 2010). The primer pairs of all genes used and the qPCR protocol for *PbenR* and *PbenA* was presented previously (Tsipa et al., 2016). qPCR analysis of promoters' kinetics was conducted in triplicate measurements for each time point.

2.4. Statistical analysis of experimental results

Two independent cultures were performed at each condition tested, while promoters' expression was measured in triplicates for each time point. For each promoter, the average expression and standard deviation was calculated. The error bars derived by dividing the standard deviation with the square root of 6 because the promoter expression at each time point was coming from two independent (biological) replicates and three qPCR internal (technical) replicates measurements. Increasing the number of independent replicates would increase the robustness of the results.

One way ANOVA (SigmaStat version 3.5, Systat Software UK Ltd, UK) was conducted to clarify significant differences in the mRNA expression profiles of all promoters. P-values were calculated through comparison of the mean mRNA expression between two given time points. The level of significance was accepted at P-values lower than 0.05.

2.5. Model analysis

Model simulation and parameter estimation were implemented in the process modelling environment gPROMS® (Process Systems Enterprise, 2014) and were computed on an Intel Core i7–2600 PC with 8 GB RAM running Windows 7.

2.5.1. Global sensitivity analysis

Global Sensitivity Analysis (GSA) identifies the most significant model parameters and initialises parameter estimation. The outputs of the model were: *Pr*, *Ps*, *Pu*, *Pm, PbenR, PbenA*, *m*-xylene, toluene and biomass. It was examined how the model's outputs are affected by the uncertainty forced through the parameter values and identified parameters crucial to the model's output (Kiparissides et al., 2009). Nominal values from the Koutinas et al. (2011) model initialised GSA. Sobol's method (Sobol, 2001) was used for GSA, while the method was implemented in Matlab and connected to gPROMS via goMATLAB. Parameter significance was calculated using sensitivity indices (SI) ranging from 0 (low significance) to 1 (high significance). It was assumed that SIs higher than 0.1 were significant (Sidoli et al., 2005). The sensitivity indexes were calculated on GUI-HDMR (Ziehn and Tomlin, 2009) Matlab package. The random samples used were 5000 and nominal values ranged ± 10% due to the intrinsic complexity of the model resulting in increased number of parameters. The time intervals examined were selected either prior or after 120 min and 420 min of culture time respectively, where the promoters' expression demonstrated more dynamic profiles. Specifically these time points were 70, 100, 130, 180, 350 and 430 min.

2.5.2. Parameter estimation in gPROMS

Parameter estimation in gPROMS is based on the Maximum Likelihood formulation, which provides simultaneous estimation of parameters in both the physical model of the process as well as the variance model of the measuring instruments. gPROMS determines values for the uncertain physical and variance model parameters, θ, that maximise the probability that the mathematical model will predict the measured values obtained from the experiments. Assuming valid independent, normally distributed measurement errors, e_{ijk}, with zero means and standard deviations, σ_{ijk}, this maximum likelihood goal can be captured through the following objective function:

$$\Phi = \frac{N}{2}\ln(2\pi) + \frac{1}{2}\min_{\theta}\left\{\sum_{i=1}^{NE}\sum_{j=1}^{NViNMij}\sum_{k=1}\left[\ln(\sigma_{ihk}^2) + \frac{(\overline{z}_{ijk} - z_{ijk})^2}{\sigma_{ihk}^2}\right]\right\}$$

where N stands for total number of measurements taken during all the experiments, θ is the set of model parameters to be estimated, NE is the number of experiments performed, NV_i is the number of variables measured in the i^{th} experiment and NM_{ij} is the number of measurements of the j^{th} variable in the i^{th} experiment. The variance of the k^{th} measurement of variable j in experiment i is denoted as σ_{ijk}^2, while z_{ijk} is the k^{th} measured value of variable j in experiment i and z_{ijk} is the k^{th} (model-) predicted value of variable j in experiment i. The above formulation can be reduced to a recursive least squares parameter estimation if no variance model for the sensor is selected. Following GSA, the parameters were estimated in gPROMS. The constant variance of experimental results at each time point was set to 0.1.

2.5.3. Statistical analysis between model(s) simulation and experimental results

The R^2 correlation of determination calculated the goodness of fit for experimentally determined: promoter expression, toluene and *m*-xylene utilisation, as well as biomass formation patterns. R^2 represents the percent of the predicted data approximated by the experimental results. In the GRN model, we evaluated R^2 vector with respect to all six promoters (*Pr*, *Ps*, *Pu*, *Pm*, *PbenR* and *PbenA*) at each time point because the promoters constitute inter-dependent elements of a complex transcriptional regulatory network. Furthermore, in the GRN-GK model, R^2 vector was evaluated with respect to mixed-substrates utilisation and biomass formation patterns because the predicted performance of the bioprocess was the main aim of microbial growth kinetics modelling.

2.6. Dynamic optimisation

The developed GRN-GK model was subject to model analysis employing GSA followed by parameter estimation at fed-batch mode (supplementary material, Table 9, 10, 11). Consequently, the optimisation of the formulated problem (supplementary material, Table 12) was performed providing the optimal substrate feeding strategy.

3. Results

3.1. Development of the dynamic hybrid GRN-growth kinetic model

A map of the paradigm targeted GRN depicting the transcriptional regulation of aromatic pollutants in *P. putida* mt-2 is shown in Fig. 2. The interacting molecular components of the GRN were implemented as a scheme of logic gates, based on the principle of biochemical

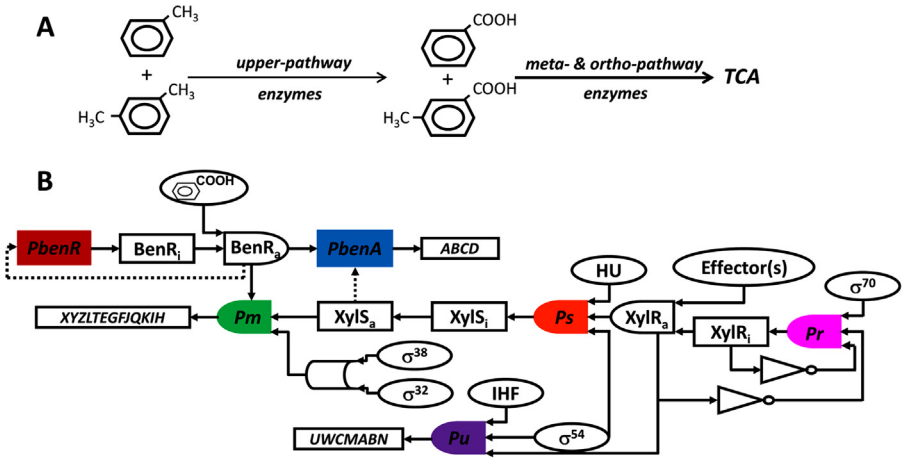

Fig. 2. The main gene regulatory network responsible for *m*-xylene and toluene transformation to tricarboxylic acid (TCA) cycle intermediates which are necessary for biomass growth. Upon induction with substrate(s) the inactive form of XylR ($XylR_i$) oligomerises forming the active molecule $XylR_a$ which activates *Pu* and *Ps* promoters. Both XylR forms down-regulate their own promoter, *Pr*. Upon *Pu* activation the *upper*–operon, encoding for the enzymes that catalyse *m*-xylene and toluene catabolism into the intermediates *m*-methyl-benzoate and benzoate respectively, is triggered. *Ps* activation and the presence of these two intermediates lead to overexpression of the *xylS* gene dimerising the inactive XylS protein to its active protein form. XylS dimerisation results in *Pm* activation that controls the *meta*-operon encoding for the enzymes further catalysing the conversion of *m*-methyl-benzoate and benzoate to TCA cycle metabolites. Benzoate is the environmental signal activating the *ortho*-cleavage regulatory network. *PbenR* controls transcription from the *benR* gene, which encodes for the BenR protein. Benzoate activates BenR which up-regulates expression from *Pm* in TOL and *PbenA* in the *ortho*-cleavage network. *PbenA* controls the *ben*-operon, which encodes for the enzymes responsible for further benzoate transformation into TCA cycle intermediates. Consequently, (A) the enzymes encoded in the *upper*-operon transform *m*-xylene and/or toluene into *m*-methyl-benzoate and benzoate, respectively. *m*-methyl-benzoate and benzoate are converted into TCA cycle metabolites through *meta*- and *ortho*- enzymes activity. The gene regulatory network with the overimposed regulation is represented as a (B) genetic circuit. ▭: input; ⊐: output; ⊓: AND; ⋈: OR; ⬭: NOT; →: potential up-regulatory mechanism.

inverters (Weiss, 2001) representing a genetic circuit in direct analogy to electronic systems. Specified combinations of the logic gates facilitate simpler descriptions of inherent regulatory loops. Hill functions were employed as input functions to the genes, enabling dynamic characterisation of bioprocess components (Alon, 2006). Despite the very complex structure of the specific genetic circuit, from a mere engineering point of view, dynamic modelling was possible facilitating in depth understanding of the network's logic (Koutinas et al., 2010). Induction of the *P. putida* mt-2 with toluene activates the TOL and chromosomal *ortho*-cleavage regulatory networks resulting in a cross-talk between the two pathways (Cowles et al., 2000). To capture dual substrate utilisation, we extended and upgraded previous work on *m*-xylene and the TOL genetic circuit (Koutinas et al., 2011) to incorporate qualitative information of the chromosomal pathway (supplementary material, Table 1).

An independent experiment was performed to assess the GRN model's structure. *P. putida* mt-2 cells were exposed to 0.7 mM of *m*-xylene and 0.7 mM of toluene. Biomass, *m*-xylene and toluene concentrations were measured until both substrates were depleted (Fig. 3A, B). The results revealed sequential substrate utilisation whereby *m*-xylene was catabolised first followed by simultaneous biodegradation of both substrates, which occurred when *m*-xylene concentration dropped below 0.2 mM (Fig. 3B). Similar utilisation of the toluene/*m*-xylene mixture has been observed (Duetz et al., 1998), although the threshold for simultaneous degradation was found to be 0.5 mM of *m*-xylene. The transcriptional kinetics of the promoters expressed was systematically evaluated through time course qPCR analysis. Specifically, the kinetic profiles of *Pr* (Fig. 3C), *Ps* (Fig. 3D), *Pu* (Fig. 3E) and *Pm* (Fig. 3F) promoters of TOL as well as the key promoters *PbenR* (Fig. 3G) and *PbenA* (Fig. 3H) of the *ortho*-cleavage regulatory network were assessed. Expression of *Pr* confirmed a down-regulatory response upon exposure to the aromatic compounds (Marques et al., 1998), while decrease in toluene concentration below a threshold level of 0.3 mM resulted in increased expression of *Pr* (Fig. 3C) (Tsipa et al., 2016).

A switch point in the response of the promoters was identified, which occurred at the 0.2 mM *m*-xylene threshold concentration that caused the onset of toluene degradation indicating the direct relationship between substrate concentration and the GRN responsible for substrate degradation. The GRN model structure was corrected to capture the observed switches and provide flexibility (supplementary material, Table 2). *Ps*, *Pu* and *Pm* (Fig. 3D-F) promoters displayed bi-modal expression due to the presence of the double substrate (Tsipa et al., 2017). During the activation/deactivation phase, expression of the promoters increased to a maximum level followed by gradual decrease ($P < 0.05$). This is potentially due to variation in the relevant expression level of the master regulator, XylR, activating directly *Pu* and *Ps*, which encode for XylS triggering expression from *Pm*. The up-regulatory response of these promoters was similar to previous studies (Marques et al., 1994; Tsipa et al., 2016) proposing a general up-regulatory response of TOL in the presence of aromatics as single- or mixed-substrates, potentially due to activation of a relevant transcription factor and subsequent de-activation. *PbenR* (Fig. 3G) and *PbenA* (Fig. 3H) were not expressed prior to the switch point (0.2 mM *m*-xylene). *Pu* controls transcription from the *upper*-operon leading to *m*-methyl-benzoate formation during *m*-xylene consumption, which does not constitute a stimulus for the *ortho*-cleavage pathway (Perez-Pantoja et al., 2015). However, below the threshold point, toluene catabolism was enabled resulting in benzoate formation through the catalytic activity of *upper*-operon enzymes. Since benzoate is known to trigger the *ortho*-cleavage regulatory network (Perez-Pantoja et al., 2015) and to strongly activate *PbenR* (Tsipa et al., 2016), an up-regulatory response of *PbenR* was expected. Nonetheless, *PbenR* was not expressed, possibly due to the presence of the multiple carbon sources (*m*-xylene and toluene) activating carbon catabolite repression (CCR) mechanisms (Tsipa et al., 2017). BenR protein serves as the transcription factor for *PbenA* and it has been suggested to be responsible for up-regulation of *PbenR* expression (Tsipa et al., 2016, 2017). Thus, the lack of *PbenR* and *PbenA* expression in the presence of *m*-xylene and toluene may be relevant to BenR repression, which is common in *P. putida* strains upon activation of CCR mechanisms (Moreno and Rojo, 2008). Following depletion of the preferred substrate, the CCR mechanisms are switched off and the cells catabolise the remaining compounds (Moreno and Rojo, 2008). The expression pattern of *PbenA* (Fig. 3H), following the switch point, was similar to those of *Ps* (Fig. 3D), *Pu* (Fig. 3E) and *Pm* (Fig. 3F) in the TOL indicating co-stimulation of the specific promoter by the XylS transcription factor of TOL (Tsipa et al., 2016).

Microbial growth kinetics was linked to GRN by focusing on the enzymatic steps of the GRN model that catalyse substrate(s) degradation and biomass growth. Upon exposure to the substrate(s), although all catabolic enzymes were produced, three enzymes were considered as rate-limiting controlling the cascades responsible for initialisation of substrate transformation (XylU) and Krebs cycle intermediates

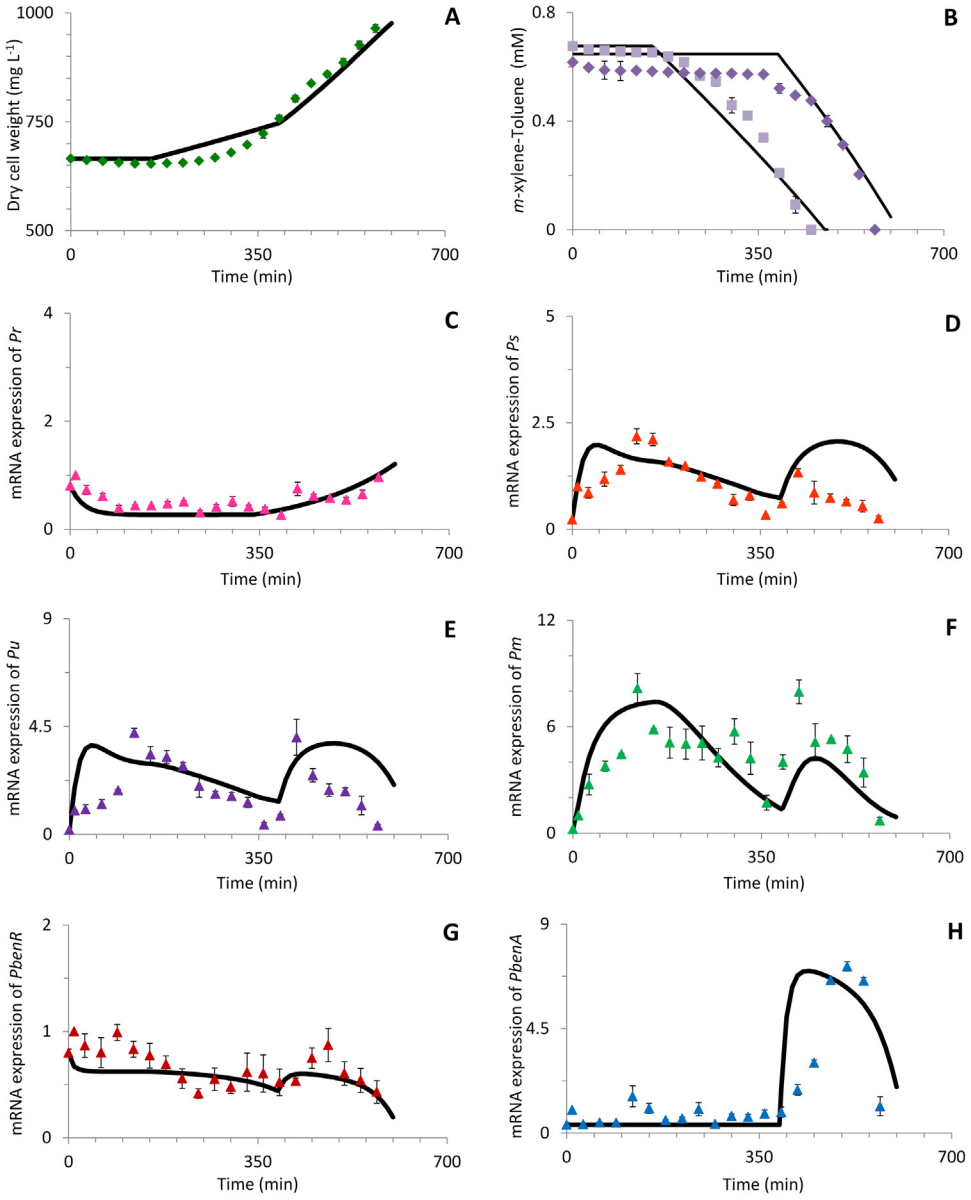

Fig. 3. Prediction of the GRN-GK model regarding biomass formulation, substrates utilisation and transcriptional kinetics of the promoters. Shown are the model simulations of parameter estimation ( ) and experimental points for A) biomass ( ), B) *m*-xylene ( ) and toluene ( ), C) *Pr* ( ), D) *Ps* ( ), E) *Pu* ( ), F) *Pm* ( ), G) *PbenR* ( ), H) *PbenA* ( ) in induction with 0.7 mM of *m*-xylene and 0.7 mM of toluene. The results for transcriptional kinetics are obtained as an average from six individual measurements at each point and the error bars are calculated for standard error. The results for substrates degradation and biomass formation are obtained as an average from two individual measurements at each point and the error bars are calculated for standard deviation.

formation, resulting in biomass growth (XylM, BenB). Production of the rate-limiting enzymes was modelled based on the GRN's genetic circuit (supplementary material, Table 1), while the microbial growth kinetics equations were constructed based on the concentration of the rate-limiting enzymes of the GRN studied. Instigated by the threshold of 0.2 mM of *m*-xylene, mathematical representation of *m*-xylene and toluene biodegradation was reformulated (supplementary material, Table 3). The parameters and variables of the hybrid GRN-GK model are presented as supplementary material (supplementary material, Tables 4, 5).

3.2. Model analysis

Model uncertainty due to parameters was allocated by model analysis employing GSA which contributes to decrease output uncertainty by accurate parameter estimation (Kiparissides et al., 2011). The results of the GSA demonstrated that 22 out of 41 parameters were important (supplementary material, Fig. 1), which incorprate biological relevance. Promoter expression is determined by the translation rate and degradation parameters of the relevant regulatory transcription factors. The significant parameter for *m*-xylene and toluene outputs is the associated maximum pollutant metabolic quotient based on XylU, which is the rate-limiting enzyme responsible for initialisation of substrate transformation controlled by *Pu*, confirming the link between substrate effectors and expression of promoters. The significant parameters for biomass output were the maximal expression of *PbenR*, *PbenA* as well as the translation rate and degradation of the rate-limiting enzyme (BenB), which is responsible for biomass formation. This GSA result underlines the necessity of extending the previous TOL genetic circuit model (Koutinas et al., 2011) to incorporate the key chromosomal *ortho*-cleavage pathway to accurately capture growth kinetics during the biodegradation of aromatics by *P. putida* mt-2. Parameter estimation was performed using the independent experiment of induction with 0.7 mM of *m*-xylene and 0.7 mM of toluene to obtain accurate values for the significant parameters (supplementary material, Tables 4, 5). As a result, the model accurately predicted biomass, toluene and *m*-xylene concentration profiles (Fig. 3A, B) as well as promoter expression profiles for *Pr* (Fig. 3C), *Ps* (Fig. 3D), *Pu* (Fig. 3E), *Pm* (Fig. 3F), *PbenR* (Fig. 3G) and *PbenA* (Fig. 3H).

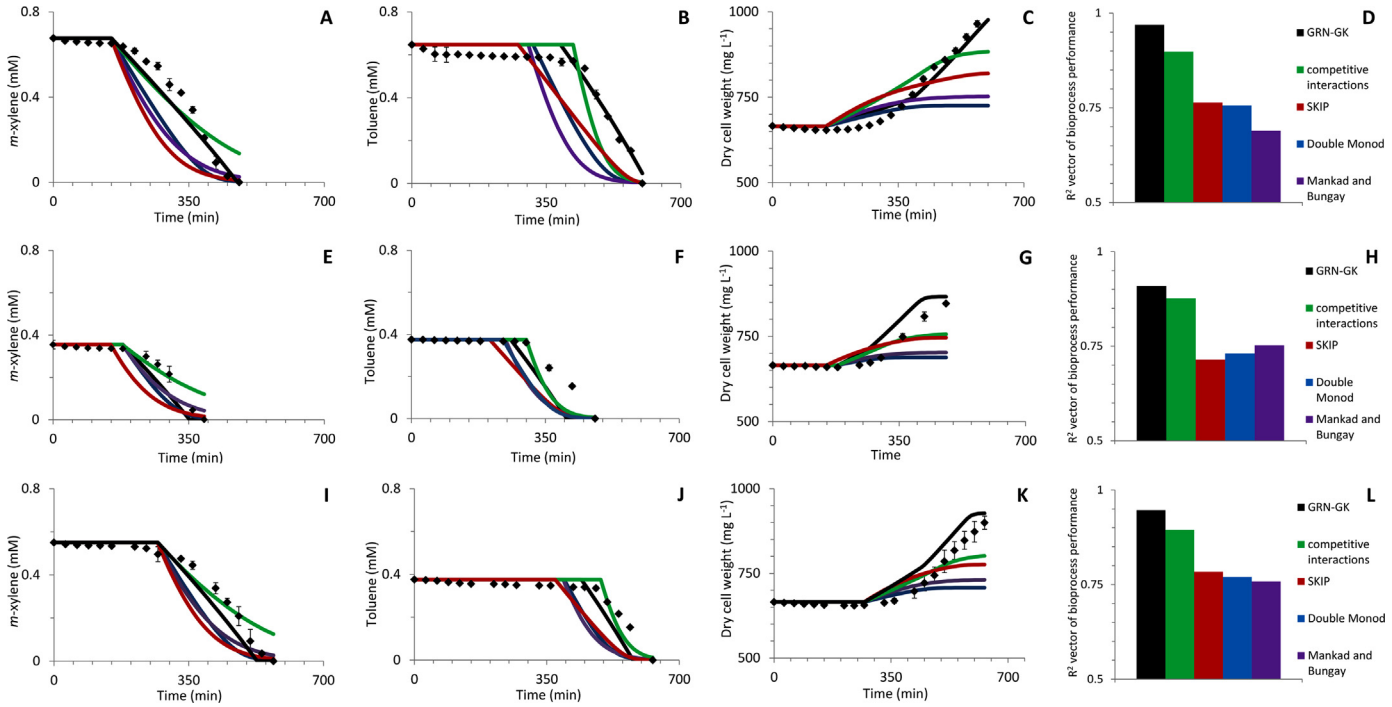

Fig. 4. Mixed-substrate and biomass growth experimental patterns (◆) predicted by: 1) the GRN-GK framework (■), 2) double Monod (■), 3) Mankad and Bungay (■), 4) competitive enzyme interactions (■) and 5) SKIP model (■). Shown are: biodegradation of (A) 0.7 mM of *m*-xylene, (B) 0.7 mM of toluene, (C) relevant biomass growth, (D) R^2 vector representing bioprocess performance; biodegradation of (E) 0.4 mM of *m*-xylene, (F) 0.4 mM of toluene, (G) relevant biomass growth, (H) R^2 vector representing bioprocess performance; biodegradation of (I) 0.6 mM of *m*-xylene, (G) 0.4 mM of toluene, (K) relevant biomass growth, (L) R^2 vector representing bioprocess performance. The results for substrates degradation and biomass formation are obtained as an average from two individual measurements at each point and the error bars are calculated for standard deviation.

3.3. Prediction of mixed-substrates growth kinetics

The accuracy of the validated GRN-GK model was assessed. The function and dynamics of promoters expression (Fig. 3C-H) were sufficiently described (average R^2 vector = 0.71; supplementary material, Table 6); the discrepancy can be explained due to the intrinsic complexity of gene regulation as well as certain model limitations. In particular, regulation of *PbenR* by BenR has been incorporated into the model based on limited experimental observations, which have not been fully validated yet (Tsipa et al., 2016). Furthermore, although the model accounted for *PbenA* expression based on BenR synthesis, it did not consider co-regulation by the TOL-encoded active form of XylS (Tsipa et al., 2016). Despite model limitations at gene regulation level, bioprocess kinetics (Fig. 3A, B) were captured more accurately (R^2 *m*-xylene = 0.96, R^2 toluene = 0.97 and R^2 biomass = 0.98; supplementary material, Table 7).

The GRN-GK model's performance was compared with common models of mixed-substrate microbial growth kinetics: (1) competitive enzyme interactions, (2) double Monod, (3) Mankad and Bungay model, and (4) the SKIP model (Yoon et al., 1977) (supplementary material, Table 8). The GRN-GK model displayed notable accuracy in predicting bioprocess performance (Fig. 4A-C; R^2 vector = 0.97) when compared to the empirical models used (R^2 vector of the competitive enzyme interactions model = 0.9, R^2 vector of the double Monod model = 0.76, R^2 vector of the Mankad and Bungay model = 0.69, and R^2 vector of the SKIP model = 0.76), as shown in Fig. 4D. Furthermore, whereas the traditional models failed to capture the biomass yield (Table 1), a crucial factor for bioprocesses design, the GRN-GK model prediction (2.4 g/g) was extremely close to the experimentally observed yield (2.3 g/g).

Mathematical models are limited by their narrow applicability. The performance of the GRN-GK model under a wide range of bioprocess conditions was evaluated: A) low pollutant concentration (0.4 mM of *m*-xylene and 0.4 mM of toluene), which may not be able to support biomass growth (Fig. 4E-G). The GRN-GK model's fidelity outperformed (R^2 vector = 0.91, Fig. 4H) the other four models (R^2 vector ranged from 0.71 to 0.88; Fig. 4H), including biomass yield prediction (Table 1). B) Induction of the *P. putida* mt-2 with different concentrations for the substrates (0.6 mM of *m*-xylene and 0.4 mM of toluene) to explore model behaviour under simulated practical conditions of varying substrate concentrations (Fig. 4I-K). The fidelity of the four models was lower (R^2 vector ranged from 0.76 to 0.89; Fig. 4L) compared to the GRN-GK model (R^2 vector = 0.96, Fig. 4L), including biomass yield (Table 1).

Table 1
Comparison of biomass yields obtained in experimental and simulated trials using different models at the initial conditions tested. Biomass yields (g of biomass per g of pollutant mixture) obtained at: A) 0.4 mM *m*-xylene-0.4 mM toluene, B) 0.6 mM *m*-xylene-0.4 mM toluene, and C) 0.7 mM *m*-xylene-0.7 mM toluene.

	A	B	C
	g biomass / g pollutant mixture		
experimental	**2.5**	**2.5**	**2.3**
GRN-GK	**2.8**	**2.8**	**2.4**
double Monod	0.3	0.5	0.5
Mankad & Bungay	0.6	0.7	0.7
competitive interactions	1.6	1.7	1.7
SKIP	1.2	1.2	1.2

3.4. Model-based gene control

The GRN-GK model was employed to design a fed-batch feeding strategy and was based on the single-substrate (toluene) model of TOL and *ortho*-cleavage promoters in *P. putida* mt-2 (Tsipa et al., 2016) (supplementary material, Table 9, 10, 11). In the presence of aromatic

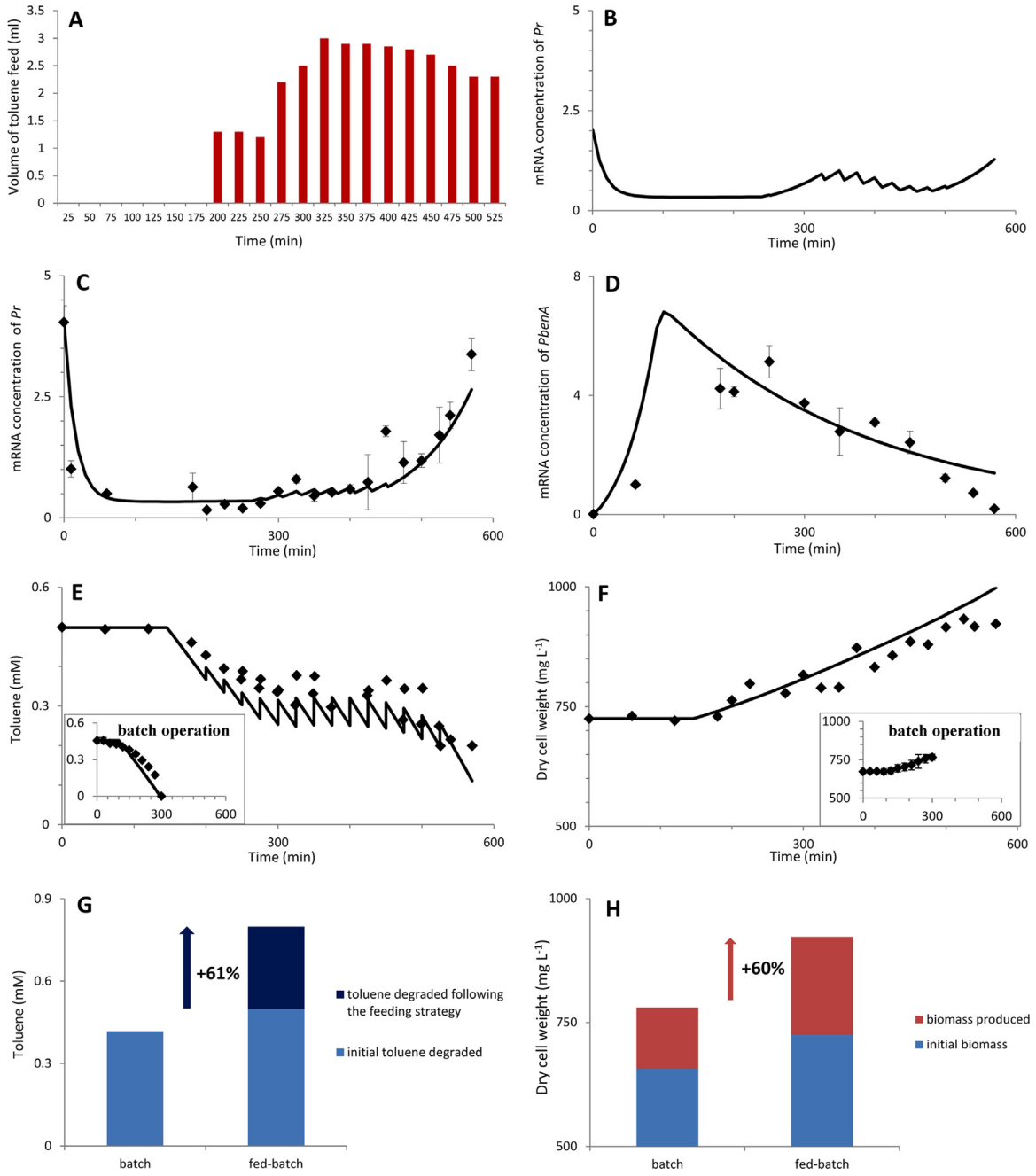

Fig. 5. Model-based gene control of the fed-batch toluene biodegradation process resulted in: (A) The optimum feeding schedule, and (B) the expression profile of *Pr*; followed by the model simulations (▬) and experimental points (◆) for: (C) *Pr* expression, (D) *PbenA* expression, (E) toluene biodegradation, (F) biomass growth at initial toluene concentration of 0.4 mM. Comparison of fed-batch and batch process at initial toluene concentration of 0.4 mM resulted in increase in the amount of (G) biodegraded toluene, (H) biomass produced upon fed-batch operation; ▬: initial, ▬: toluene degraded following the model-based feeding strategy, ▬: biomass produced. The results for transcriptional kinetics are obtained as an average from three individual measurements at each point and the error bars are calculated for standard deviation.

effectors, the constitutively expressed *Pr* is the first promoter expressed in the TOL metabolic pathway triggering subsequent metabolic activities that render its function the core element in the TOL as well as in every interlinked metabolic pathway relevant to the biodegradation of pollutants. *P. putida* mt-2 induction with a TOL effector results in down-regulatory response of *Pr* which is also involved in a negative feedback loop leading to optimised function of the TOL plasmid providing inbuilt stability (Becskei and Serrano, 2000). An optimal fed-batch feeding strategy profile was designed *in silico* (Fig. 5A) at an initial toluene concentration of 0.4 mM formulating a dynamic optimisation problem of controlling *Pr* expression to be maintained at a level close to 0.5 (Fig. 5B). Close to this level, *Pr* is down-regulated participating in the negative feedback loop, whereas above this level *Pr* expression increases (Tsipa et al., 2016). As previously observed, this increase occurs below 0.3 mM toluene concentration (Tsipa et al., 2016). Therefore, when *Pr* level exceeds 0.5, toluene concentration is below 0.3 mM. Consequently, re-activation of the *Pr* down-regulatory response is required by additional toluene that maximises toluene biodegradation rate leading to *Pr* expression decrease close to 0.5 (supplementary material, Table 12). The model-based gene control enabled prediction of substrate consumption, the transcriptional kinetics of promoters in the TOL and *ortho*-cleavage pathway as well as biomass growth at fed-

batch mode. The TOL and *ortho*-cleavage promoter expression were adequately modelled (TOL-*Pr* R^2 = 0.82, *ortho*-cleavage-*PbenA* R^2 = 0.77; Fig. 5C, D) considering the intrinsic GRN complexity and certain model limitations, as explained above. Furthermore, accurate prediction of toluene biodegradation (R^2 =0.82) and biomass formation (R^2 =0.93) kinetic patterns (Fig. 5E, F), was observed. Accordingly, the gene-based feeding strategy of the pollutant in the fed-batch experiment resulted in significant increase in toluene biodegradation (23%; Fig. 5G) and biomass formation (58%; Fig. 5H), as compared to the batch culture conducted at the same initial toluene concentration.

4. Discussion

Herein, a novel hybrid framework has been developed that connects targeted GRN modelling to growth kinetics for bioprocess design and optimisation. The framework: (a) demonstrated quantitative control of a targeted complex regulatory network, (b) achieved systematic representation of substrate(s) metabolism, (c) enabled accurate prediction of bioprocess performance and biomass yield, (d) efficiently predicted mixed-substrate growth kinetics under several conditions, and (e) was compared against other commonly applied models demonstrating superior performance. The model-based control achieved at the gene level serves as a proof-of-concept to evaluate the application of engineering approaches for direct re-programming of cellular activity that either avoids strain manipulation or used for enhancing robustness on synthetic genetic circuit design (Nielsen et al., 2016) similarly to control engineering strategies (He et al., 2016).

Bioprocess optimisation requires accurate monitoring and estimation of critical bioprocess parameters, such as specific growth rate, substrate utilisation, and biomass and/or product formation rates. Currently, the 70-year old Monod (and Monod-type) kinetic models are being universally used in biotechnology and systems biology despite being empirical and treat the bioprocess as a 'black box' while omitting gene regulatory mechanisms. Consequently, they lack of predictability over a broad range of conditions. Furthermore, mixed substrate model development has stagnated; Monod-type models assume competition or parallel substrate utilisation (Yoon et al., 1977) based on unspecified substrate inhibition while ignoring that specific gene regulatory networks control substrate transformation and biomass/product formation. Over the last 25 years, modelling approaches such as cybernetic (Ramakrishna et al., 1997) and structured models (Nikolajsen et al., 1991), which are mainly based on enzyme level control and built under steady state assumptions, have not yielded significant progress. In contrast, the GRN-GK framework demonstrated that double-substrate degradation proceeds through the same metabolic pathway/gene regulatory network whereby the preferred substrate (*m*-xylene), which is more methylated, induced the first regulatory response of the TOL and *ortho*-cleavage promoters followed by the second regulatory response due to the other non-preferred substrate (toluene), which is less methylated. This bi-modal promoter behaviour specified the threshold switch point of substrate utilisation. As a result, the platform accurately predicted mixed-substrate bioprocess performance and biomass yield under a wide range of operating conditions. Consequently, the GRN-GK framework can be applied to elucidate fundamental problems associated with the prediction of real process phenomena such as substrate (s) availability and fluctuating pollutant loads (Koutinas et al., 2007a, b) enhancing bioremediation or production of bio-based commodities.

Feeding strategy optimisation of fed-batch bioprocesses is essential in bioremediation and industrial-scale life sciences and biotechnology applications. Fed-batch feeding strategy scheduling is currently optimised either experimentally or through model-based optimisation; the latter conducted by performing stochastic or deterministic dynamic optimisation (Banga et al., 2005) on empirical growth kinetics models through maximisation of a performance index, commonly being biomass productivity (De la Hoz Siegler et al., 2012; Kiparissides et al., 2015; Mozumdera et al., 2014) or an economic index based on the operation profile and final concentrations (Banga et al., 2005). The GRN-GK framework proposes an exciting new approach to the feeding strategy optimisation of fed-batch systems by performing deterministic dynamic optimisation through control of the performance of a key promoter, which regulates substrate degradation and biomass formation. Consequently, optimal feeding strategy was achieved by maintaining constant gene activity avoiding unnecessary substrate depletion in contrast to the traditional fed-batch optimisation strategies that feed substrate just prior to the substrate being depleted.

The interconnected fields of systems and synthetic biology have provided new avenues in biotechnology and biomedicine (Campbell et al., 2017; Ellis et al., 2009) and aim to become applicable in biotechnology and industrial bioprocessing (Campbell et al., 2017); however, their applicability in industrial bioprocesses is currently limited. Systems biology approaches generate large information datasets regarding the phenotypic and physiological characteristics of the microorganisms. However, global modelling of gene regulatory networks is challenging due to: (1) the excessive detail of genome annotation, which is constantly updated and refined to incorporate new genome-based knowledge (Campbell et al., 2017); (2) the large number of possible solutions explaining equally the problem of which only one can be biologically relevant (De Smet and Marchal, 2010); (3) incorrect prediction of regulatory interactions between a transcription factor(s) and target genes (Marbach et al., 2012); (4) simplifying model assumptions profoundly affecting accuracy (Marbach et al., 2010); and assuming steady-state conditions (Park et al., 2011). In contrast, the GRN-GK framework follows a targeted approach to capturing biological behaviour of complex gene regulatory networks (Koutinas et al., 2010) by focusing on the main metabolic pathway of *P. putida* mt-2 activated upon exposure to mixed-substrates. By utilising consistent, systematic time-series data of specific promoter(s) mRNA expression and subsequently efficiently connecting it to growth kinetics, an accurate, dynamic, experimentally-validated, computationally tractable, and predictive model was developed capable of capturing mixed-substrates and growth patterns of industrially-relevant bioprocesses. Whereas genome-scale models are unable to represent time-scale changes, such as promoter activation that occurs within minutes, and environmental changes, such as substrates fluctuation, the GRN-GK framework is capable of identifying threshold switch point(s) of mixed-substrate utilisation thus representing a systematic optimal bioprocess design tool in industrial bioprocessing. Therefore, this framework may constitute a practical complementary approach to systems and synthetic biology.

GSA of the GRN-GK model revealed significant parameters associated with promoter expression, substrate utilisation (confirming the link between substrate effectors and expression of promoters), and biomass formation. The importance of this mathematical analysis is that the identified significant parameters incorprate biological relevance. Specifically, based on GSA results if the binding site of XylRa on *Pu* or that of BenRa on *Pm* was modified the biodegradation of aromatics would be significantly affected. Therefore, GSA analysis could prove to be a valuable tool for model-driven strain modifications apart from systems genetic or metabolic engineering model-based approaches employed for strain optimisation (Lee and Kim, 2015; Ranganathan et al., 2010).

Acknowledgements

This work was supported by the EC FP7-funded Marie Curie initial training network MULTIMOD [Project Number 226462, 207–2013]. The authors would like to thank Prof. Victor de Lorenzo for kindly providing *P. putida* mt-2 strain.

Appendix A. Supplementary material

Supplementary data associated with this article can be found in the online version at http://dx.doi.org/10.1016/j.ymben.2018.04.023.

References

Akesson, M., Forster, J., Nielsen, J., 2004. Integration of gene expression data into genome-scale metabolic models. Metab. Eng. 6, 285–293.

Almquist, J., Cvijovic, M., Hatzimanikatis, V., Nielsen, J., Jirstrand, M., 2014. Kinetic models in industrial biotechnology – Improving cell factory performance. Metab. Eng. 24, 38–60.

Alon, U., 2006. An Introduction to Systems Biology: Design Principles of Biological Circuits. CRC Press, Florida.

Aranda-Olmedo, I., Ramos, J.L., Marques, S., 2005. Integration of signals through Crc and PtsN in catabolite repression of *Pseudomonas putida* TOL plasmid pWW0. Appl. Environ. Microbiol. 71, 4191–4198.

Banf, M., Rhee, S.Y., 2017. Computational inference of gene regulatory networks: approaches, limitations and opportunities. BBA-Gene Regul. Mech. 1860, 41–52.

Banga, J.R., Balsa-Canto, E., Moles, C.G., Alonso, A.A., 2005. Dynamic optimization of bioprocesses: efficient and robust numerical strategies. J. Biotechnol. 117, 407–419.

Bartocci, E., Lió, P., 2016. Computational modeling, formal analysis, and tools for systems biology. PLoS Comput. Biol. 12, e1004591.

Becskei, A., Serrano, L., 2000. Engineering stability in gene networks by autoregulation. Nature 405, 590–593.

Campbell, K., Xia, J., Nielsen, J., 2017. The Impact of Systems Biology on Bioprocessing. Trends Biotechnol.

Chakrabarti, A., Miskovic, L., Soh, K.C., Hatzimanikatis, V., 2013. Towards kinetic modeling of genome-scale metabolic networks without sacrificing stoichiometric, thermodynamic and physiological constraints. Biotechnol. J. 8, 1043–1057.

Cowles, C.E., Nichols, N.N., Harwood, C.S., 2000. BenR, a XylS Homologue, regulates three different pathways of aromatic acid degradation in *Pseudomonas putida*. J. Bacteriol. 182, 6339–6346.

De la Hoz Siegler, H., McCaffrey, W.C., Burrell, R.E., Ben-Zvi, A., 2012. Optimization of microalgal productivity using an adaptive, non-linear model based strategy. Bioresour. Technol. 104, 537–546.

De Smet, R., Marchal, K., 2010. Advantages and limitations of current network inference methods. Nat. Rev. Microbiol. 8, 717–729.

Duetz, W.A., Wind, B., van Andel, J.G., Barnes, M.R., Williams, P.A., Rutgers, M., 1998. Biodegradation kinetics of toluene, m-xylene, p-xylene and their intermediates through the upper TOL pathway in Pseudomonas putida (pWWO). Microbiology 144, 1669–1675.

Ellis, T., Wang, X., Collins, J.J., 2009. Diversity-based, model-guided construction of synthetic gene networks with predicted functions. Nat. Biotechnol. 27, 465–471.

Gerstl, M.P., Klamt, S., Jungreuthmayer, C., Zanghellini, J., 2016. Exact quantification of cellular robustness in genome-scale metabolic networks. Bioinformatics 32, 730–737.

He, F., Murabito, E., Westerhoff, H.V., 2016. Synthetic biology and regulatory networks: where metabolic systems biology meets control engineering. J. R. Soc. Interface 13, 20151046.

Jamshidi, N., Palsson, B.Ø., 2008. Formulating genome-scale kinetic models in the post-genome era. Mol. Syst. Biol. 4, 1–10.

Kiparissides, A., Koutinas, M., Kontoravdi, C., Mantalaris, A., Pistikopoulos, E.N., 2011. 'Closing the loop' in biological systems modeling — From the in silico to the in vitro. Automatica 47, 1147–1155.

Kiparissides, A., Kucherenko, S.S., Mantalaris, A., Pistikopoulos, E.N., 2009. Global sensitivity analysis challenges in biological systems modeling. Ind. Eng. Chem. Res. 48, 7168–7180.

Kiparissides, A., Pistikopoulos, E.N., Mantalaris, A., 2015. On the model-based optimization of secreting mammalian cell (GS-NS0) cultures. Biotech. Bioeng. 112, 536–548.

Klecka, G.M., Maier, W.J., 1988. Kinetics of microbial growth on mixtures of pentachlorophenol and chlorinated aromatic compounds. Biotechnol. Bioeng. 31, 328–335.

Koutinas, M., Baptista, I.I.R., Meniconi, A., Peeva, L., Mantalaris, A., Castro, P.M.L., Livingston, A.G., 2007a. The use of an oil-absorber-bioscrubber system during biodegradation of sequentially alternating loadings of 1,2-dichloroethane and fluorobenzene in a waste gas. Chem. Eng. Sci. 62, 5989–6001.

Koutinas, M., Baptista, I.I.R., Peeva, L.G., Ferreira Jorge, R.M., Livingston, A.G., 2007b. The use of an oil absorber as a strategy to overcome starvation periods in degrading 1,2-dichloroethane in waste gas. Biotechnol. Bioeng. 96, 673–686.

Koutinas, M., Kiparissides, A., Silva-Rocha, R., Lam, M., dos Santos, V.A.P.M., de Lorenzo, V., Pistikopoulos, E.N., Mantalaris, A., 2011. Linking genes to microbial growth kinetics: an integrated biochemical systems engineering approach. Metab. Eng. 13, 401–413.

Koutinas, M., Lam, M.C., Kiparissides, A., Silva-Rocha, R., Godinho, M., Livingston, A.G., Pistikopoulos, E.N., de Lorenzo, V., dos Santos, V.A.P.M., Mantalaris, A., 2010. The regulatory logic of *m*-xylene biodegradation by *Pseudomonas putida* mt-2 exposed by dynamic modelling of the principal node *Ps/Pr* of the TOL plasmid. Environ. Microbiol. 12, 1705–1718.

Kovarova-Kovara, K., Egli, T., 1998. Growth kinetics of suspended microbial cells: from single-substrate-controlled growth to mixed-substrate kinetics. Microbiol. Mol. Biol. R. 62, 646–666.

Lee, S.Y., Kim, H.U., 2015. Systems strategies for developing industrial microbial strains. Nat. Biotechnol. 33, 1061–1072.

Lee, W.C., Huang, C.T., 2000. Modeling of ethanol fermentation using Zymomonas mobilis ATCC 10988 grown on the media containing glucose and fructose. Biochem. Eng. J. 4, 217–227.

Marbach, D., Costello, J.C., Küffner, R., Vega, N.M., Prill, R.J., Camacho, D.M., Allison, K.R., The DREAM5 Consortium, Kellis, M., Collins, J.J., Stolovitzky, G., 2012. Wisdom of crowds for robust gene network inference. Nat. Methods 9, 796–804.

Marbach, D., Prill, R.J., Schaffter, T., Mattiussi, C., Floreano, D., Stolovitzky, G., 2010. Revealing strengths and weaknesses of methods for gene network inference. PNAS 107, 6286–6291.

Marques, S., Gallegos, M.T., Manzanera, M., Holtel, A., Timmis, K.N., Ramos, J.L., 1998. Activation and repression of transcription at the double tandem divergent promoters for the *xylR* and *xylS* genes of the TOL plasmid of *Pseudomonas putida*. J. Bacteriol. 180, 2889–2894.

Marques, S., Holtel, A., Timmis, K.N., Ramos, J.L., 1994. Transcriptional induction kinetics from the promoters of the catabolic pathways of TOL plasmid pWW0 of *Pseudomonas putida* for metabolism of aromatics. J. Bacteriol. 176, 2517–2524.

Monod, J., 1949. The growth of bacterial cultures. Annu. Rev. Microbiol. 3, 371–394.

Moreno, R., Rojo, F., 2008. The Target for the *Pseudomonas putida* Crc global regulator in the benzoate degradation pathway is the BenR transcriptional regulator. J. Bacteriol. 190, 1539–1545.

Mozumdera, M.S.I., De Wever, H., Volcke, E.I.P., Garcia-Gonzalez, L., 2014. A robust fed-batch feeding strategy independent of the carbon source for optimal polyhydroxybutyrate production. Process Biochem. 49, 365–373.

Nielsen, A.A.K., Der, B.S., Shin, J., Vaidyanathan, P., Paralanov, V., Strychalski, E.A., Ross, D., Densmore, D., Voigt, C.A., 2016. Genetic circuit design automation. Science 352, aac7341.

Nikolajsen, K., Nielsen, J., Villadsen, J., 1991. Structured modeling of a microbial system. III. growth on mixed substrates. Biotechnol. Bioeng. 38, 24–29.

O'Brien, E.J., Lerman, J.A., Chang, R.L., Hyduke, D.R., Palsson, B.Ø., 2013. Genome-scale models of metabolism and gene expression extend and refine growth phenotype prediction. Mol. Syst. Biol. 9, 1–13.

Park, J.H., Kim, T.Y., Lee, K.H., Lee, S.Y., 2011. Fed-batch culture of *Escherichia coli* for L-valine production based on *in silico* flux response analysis. Biotech. Bioeng. 108, 934–946.

Perez-Pantoja, D., Kim, J., Silva-Rocha, R., de Lorenzo, V., 2015. The differential response of the *Pben* promoter of Pseudomonas putida mt-2 to BenR and XylS prevents metabolic conflicts in *m*-xylene biodegradation. Environ. Microbiol. 17, 64–75.

Ramakrishna, R., Ramkrishna, D., Konopka, A.E., 1997. Microbial growth on substitutable substrates: characterizing the consumer-resource relationship. Biotechnol. Bioeng. 54, 77–90.

Ramos, J.L., Marques, S., Timmis, K.N., 1997. Transcriptional control of the *Pseudomonas* TOL plasmid catabolic operons is achieved through an interplay of host factors and plasmid-encoded regulators. Annu. Rev. Microbiol. 51, 341–372.

Ranganathan, S., Suthers, P.F., Maranas, C.D., 2010. OptForce: an optimization procedure for identifying all genetic manipulations leading to targeted overproductions. PLoS Comput. Biol. 6, e1000744.

Sambrook, J., Fritsch, E.F., Maniatis, E., 1989. Molecular Cloning: a Laboratory Manual. Cold Spring Harbour Press, New York.

Sidoli, F.R., Mantalaris, A., Asprey, S.P., 2005. Toward Global Parametric Estimability of a Large-Scale Kinetic Single-Cell Model for Mammalian Cell Cultures. Ind. Eng. Chem. Res. 44, 868–878.

Sławek, J., Arodz, T., 2013. ENNET: inferring large gene regulatory networks from expression data using gradient boosting. BMC Syst. Biol. 7, 106.

Sobol, I.M., 2001. Global sensitivity indices for nonlinear mathematical models and their Monte Carlo estimates. Math. Comput. Simul. 55, 271–280.

Timmis, K.N., 2002. *Pseudomonas putida*: a cosmopolitan opportunist par excellence. Environ. Microbiol. 4, 779–781.

Tsipa, A., Koutinas, M., Pistikopoulos, E.N., Mantalaris, A., 2016. Transcriptional kinetics of the cross-talk between the *ortho*-cleavage and TOL pathways of toluene biodegradation in *Pseudomonas putida* mt-2. J. Biotechnol. 228, 112–123.

Tsipa, A., Koutinas, M., Vernardis, S.I., Mantalaris, A., 2017. The impact of succinate trace on pWW0 and *ortho*-cleavage pathway transcription in *Pseudomonas putida* mt-2 during toluene biodegradation. Bioresour. Technol. 234, 397–405.

Weiss, R., 2001. Cellular computation and communications using engineered genetic regulatory networks. MIT, USA, Cambridge.

Yano, T., Koga, S., 1969. Dynamic behavior of the chemostat subject to substrate inhibition. Biotechnol. Bioeng. 11, 139–153.

Yoon, Y., Klinzing, G., Blanch, W., 1977. Competition for mixed substrates by microbial populations. Biotech. Bioeng. 19, 1193–1210.

Ziehn, T., Tomlin, A.S., 2009. GUI-HDMR—a software tool for global sensitivity analysis of complex models. Environ. Model. Softw. 24, 775–785.